STRUCTURE AND FUNCTION OF THE ESKAPE PATHOGEN GROESL CHAPERONINS

By

ILIYA VITALIEVICH PANFILENKO

_____

A Thesis Submitted to the Honors College

In Partial Fulfillment of the Bachelors degree
With Honors in

Molecular and Cellular Biology

THE UNIVERSITY OF ARIZONA

DECEMBER 2019

Approved by:

_____

Dr. Eli Chapman
Department of Pharmacology and Toxicology

ABSTRACT

GroESL is an essential bacterial chaperone system comprising the homotetradecameric, double ring GroEL and the homoheptameric cochaperone GroES that is highly conserved from bacteria to man. This class of chaperonins (large, double ring chaperones are called chaperonins) uses ATP binding and hydrolysis to fold nascent or stress denatured polypeptides into their appropriate native conformations. *E. coli* GroESL has been shown to be the only chaperone system required for organismal growth and viability under all conditions and thus has been posited as a potential antibiotic target. To date, nearly all functional studies have been carried out in *E. coli* GroESL and it has been assumed this is a viable surrogate for other bacterial GroESLs. In this work, we show that despite high GroESL sequence identity between *E. coli* and the ESKAPE pathogens, there are distinct structural and functional differences that were previously unappreciated. This observation may have critical implications for the development of small molecule inhibitors to target GroESL folding function. Attempted expression of the GroESL chaperonin complex native to each ESKAPE pathogen in *E. coli* unveiled that only *K. pneumonia*, *A. baumannii*, and *E. cloacae* were capable of rescuing GroESL deficient LG6 (lac regulated chromosomal *groESL*). More thorough evaluation of these strains revealed that *P. auruginosa*, *E. faecium*, and *S.*

aureus had a dominant negative effect when expressed in LG6. To circumvent this, we employed two distinct genetic strategies to generate an *E. coli* strain in which native GroESL could be replaced with ESKAPE GroEL without the potential for translation of both ESKAPE and *E. coli* GroEL: one with chromosomal GroEL removed, but contains a GroEL plasmid capable of negative selection, and the other where chromosomal *E. coli groESL* was replaced by ESKAPE *groESL*. We found that all of the ESKAPE chaperonins could compliment in the clean genetic background, except for *S. aureus*. Using a series of chimeras, we identified which GroEL domains from *P. auruginosa* and *E. faecium* may have been responsible for the observed dominant negative effect in the presence of *E. coli* GroEL. Coexpression of *P. auruginosa/E.coli* or *E. faecium/E.coli* GroEL produced mixed tetradecamers. The chaperonins generated by this method exhibited diminished ATPase activity, suggesting compromised chaperoning ability. The results of our studies suggest that the expression of GroESL in nonnative organisms may be affected by the formation of hypofunctional mixed rings as a consequence of allosteric differences which are to be further investigated.

INTRODUCTION

In the United States, approximately 2 million people become infected with antibiotic resistant bacteria each year. Notably, healthcare-associated multidrug-

resistant infections cause 99,000 deaths per year within the U.S..[1] The primary bacterial culprits identified as causes of these infections are ***E****nterococcus faecium*, ***S****taphylococcus aureus*, ***K****lebsiella pneumoniae,* ***A****cinetobacter baumannii*, ***P****seudomonas aeruginosa* and ***E****nterobacter* spp. Collectively, these organisms are known as the **ESKAPE** pathogens. It is projected that close to 10 million individuals will die from antibiotic resistant infections annually involving these and other pathogens by 2050.[2] The severity of disease which these organisms impose on infected individuals is reflected not only by their clinical pathogenicity but also the burden of treatment costs to society. In the United States alone, total yearly spending associated with the treatment of antibiotic resistant bacteria is approximately $20 billion.[3] Although me-too antibiotics are produced and marketed each year, infectious bacteria quickly develop mechanisms of antibiotic avoidance against these agents. The ongoing lethality, economic impact, projected future loss of human life, and adaptability to newly marketed antimicrobial medicines associated with antibiotic resistant organisms collectively highlight the urgent need for the development of antibacterial drugs with novel modes of action. If the surge of antibiotic-resistant infections contributing to the aforementioned issues are to be circumvented, previously overlooked bacterial drug targets which can eliminate or slow the growth of bacteria must be considered.

One potential target for novel antibiotics, conserved among all of the ESKAPE pathogens is the GroEL/ES chaperonin system. GroESL is essential for bacterial growth under all conditions. GroEL uses the energy of ATP-binding and hydrolysis to fold newly translated or stress denatured polypeptides into functional structures. As noted by a multitude of previous studies, GroEL is the only chaperone who's proper function is absolutely essential to bacterial growth and survival at all temperatures.[4] GroEL is a homotetradecamer that forms two rings of seven subunits stacked back-to-back (Fig.1). Each subunit has an equatorial domain, an apical domain, and an intermediate domain. GroES is the homoheptameric cochaperone of GroEL, which behaves as a molecular lid, binding to the apical domains of the GroEL *cis* ring and enclosing the respective cavity during polypeptide refolding. At the start of a typical chaperoning cycle, an incompletely folded or misfolded polypeptide binds to a hydrophobic region at the apical domain of the *cis* ring (Fig.2, Step 1).[5] Hydrophobic and electrostatic interactions between the hydrophobic amino acid residues of the polypeptide and those comprising the apical domain facilitate this binding. Next, seven molecules of ATP are rapidly and cooperatively bound by GroEL at the seven sites of the *cis* ring ring[6]. Owing to the anticooperative behavior of the *cis* and *trans* rings of

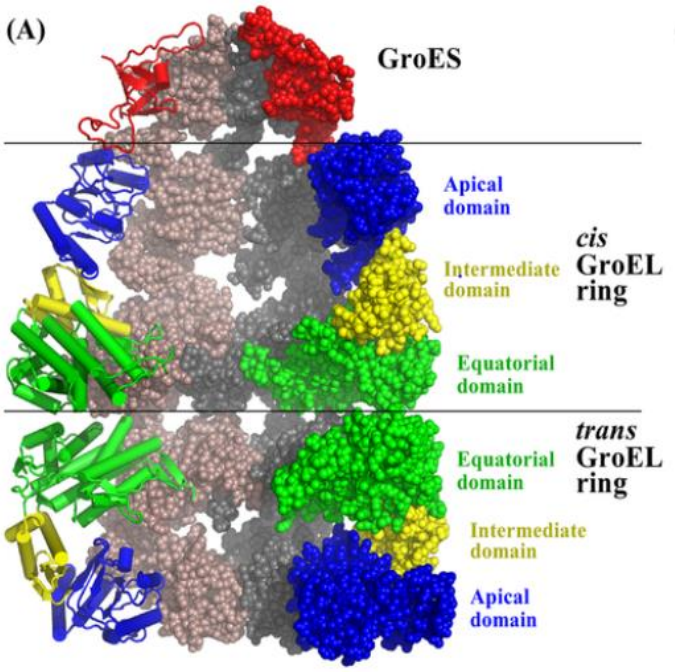

Figure 1. GroEL exhibits a homotetradecameric structure comprised principally by a *cis* ring and a *trans* ring. Both rings are constituted by seven subunits. Each subunit is comprised by an apical domain, an intermediate domain, and an equatorial domain. GroES is a homoheptameric cochaperone that acts as a molecular lid, positioning itself onto the apex of the *cis* ring during polypeptide folding.

GroEL, only one ring will be occupied with ATP at a time under physiological conditions.[6] ATP binding to the equatorial domains of the open *cis* ring promotes a modest elevation and 30° counterclockwise swivel of the apical domains bound to the polypeptide.[6] This allostery-dependent structural change makes the apical domains competent to bind GroES.[6] GroES is then recruited to the apical domains of the cis-ring where it closes the polypeptide-containing cavity, encapsulating the substrate of interest within the chaperonin (Fig, 2, Step 2).[5] Importantly, GroES is incapable of binding to and capping GroEL in the absence of ATP.[5] GroES binding to the apical domains of the *cis* ring causes the apical domains to undergo significant rigid body motion, rotating them clockwise by 120° and elevating them by 60°.[6,7,8] These structural rearrangements allow for the removal of the hydrophobic substrate from its previous binding sites and

release of the polypeptide into the hydrophilic central cavity of the *cis* ring.[6] Altogether, the median polypeptide binding chamber undergoes a 2-fold expansion.[5] This expansion serves to accommodate the polypeptide while it undergoes refolding (Step 3).[5,6] The folding phase is the most protracted part of the GroESL folding cycle, lasting for approximately 10 seconds. During this time the chaperonin rapidly hydrolyzes ATP molecules bound to the *cis* ring, generating ADP in the process. After 10 seconds, ATP hydrolysis begins to significantly reduce GroEL-GroES binding affinity and allows for the entry of ATP into ATP-binding sites localized to the equatorial domains of the trans-ring[6,9]. Binding of ATP to the trans-ring produces an allosteric signal that promotes the release of GroES and ADP from the *cis* ring and the liberation of the folded polypeptide into the cytosol (Fig. 2, Step 4).[6] As a result, the *trans* ring ascertains the roles of the *cis* ring, becoming receptive to ATP dependent activation, GroES binding, and execution of a subsequent round of the polypeptide refolding cycle.[5] In this manner, the *cis* and *trans* rings repeatedly exchange the labor of folding with one another, exploiting ATP binding and hydrolysis as a means to relieve the previously folding-active ring from its activities while promoting nucleation of its opposing counterpart.[6]

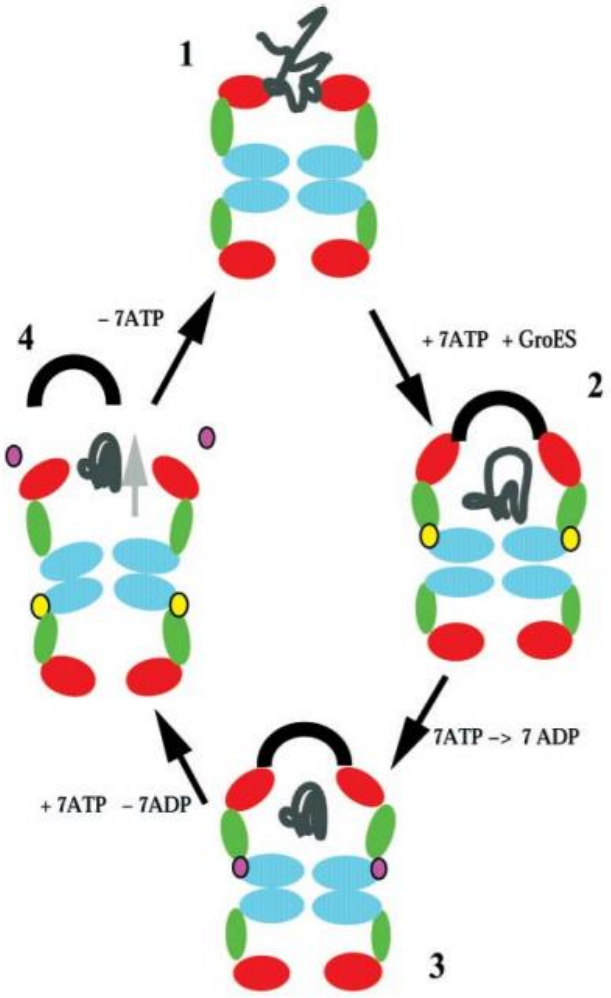

Figure 2. Schematic representation of the GroESL refolding cycle. Blue, green, and red regions correspond to the equatorial, intermediate and apical domains of the chaperonin's subunits, respectively. GroES is represented by the black half-circle. ATP and ADP are represented in yellow and magenta respectively. In Step 1 of the cycle, a nascent polypeptide is bound to the apical domains of GroEL. In step 2, 7 molecules of ATP bind to the equatorial domains of the chaperonin's *cis* ring, promoting the enlargement and encapsulation of the respective polypeptide-housing cavity. In step 3, ATP is hydrolyzed as the nascent polypeptide is folded into its mature form. In step 4, ATP binding to the *trans* ring promotes the release of GroES and the completely or partially folded polypeptide from GroEL into the cytosol, re-initiating the folding cycle.

Although previous studies have revealed that certain molecules designed by our collaborators at Indiana University (to circumvent bacterial antibiotic resistance mechanisms by targeting the GroESL system) can penetrate gram negative cells, detailed GroESL inhibition has yet to be observed using ESKAPE GroESL. In order to establish biochemical support for small molecule interaction with the target chaperonin, we elected to produce GroEL from each of the ESKAPE pathogens in LG6, a GroESL

deficient cell line. In attempting to express and purify ESKAPE GroESL produced within this strain, we discovered a dominant negative phenotype suspected to be due to the formation of hypoactive mixed complexes (native and nonnative). To overcome this observed effect, we utilized several systems to eliminate the possibility of GroEL ring-mixing between organisms. We decided to investigate this surprising result with hopes of identifying a method by which ESKAPE GroESL could be expressed and purified to enhance our understanding of the structural and functional differences between ESKAPE pathogens and *E. Coli* groESL.

RESULTS

E. faecium, S. aureus, and P. aeruginosa GroESL Are Unable to Rescue GroESL-Deficient *E. coli* Strain, LG6.

In LG6 (Cam^R), an MG1655 derived strain with *lac*-regulated *groESL* operon, pBAD promoted plasmids (Kan^R) containing *groESL* from the ESKAPE pathogens were individually transformed to evaluate the ability of each to rescue this GroESL-deficient *E. coli* system.[10] It was expected that organism rescue would only occur if the introduction of nonnative *groESL* into *E. coli* was complementary to the existing *E. coli* GroESL native to these cells. Additionally, leak from the *lac* promoter in untransformed LG6 generally appeared to be insufficient to produce colonies at high dilutions. We hypothesized that GroESL from the ESKAPE pathogens would be able to rescue

GroESL deficient LG6. This suspicion was predicated on the fact that GroES and GroEL amino acid sequence, isoelectric point, and size (residue number) were similar in all ESKAPE pathogens when juxtaposed against MG1655 (Table 1).

Bacteria	Gram Stain	GroES kDa/Residue #	GroES Identity/Similarity %	GroES PI	GroEL kDa/Residue #	GroEL Identity/Similarity %	GroEL PI
Enterococcus faecium ATCC 51559	Gram Positive	10.0/94	46.4/62.9	5.03	57.2/541	60.6/77.4	4.66
Staphylococcus aureus ATCC 25923	Gram Positive	10.4/94	43.3/62.9	4.87	57.6/538	57.1/75.8	4.56
Klebsiella pneumonia ATCC 700603	Gram Negative	10.4/97	92.8/97.9	5.38	57.1/548	96.4/98	4.84
Acinetobacter baumannii ATCC 19606	Gram Negative	10.1/96	60.2/78.6	5.09	57.1/544	75.4/86.7	4.92
Pseudomonas aeruginosa ATCC 47085	Gram Negative	10.26/97	60.8/78.4	5.17	57.1/547	79.6/88.9	5.04
Enterobacter cloacae ATCC 13047	Gram Negative	10.4/97	93.8/97.9	5.38	57.1/548	96.2/98	4.85
Escherichia coli MG1655	Gram Negative	10.4/97	-/-	5.15	57.3/548	-/-	4.85

Table 1. ESKAPE pathogen GroES/EL is predicted to be structurally similar with like net charge in their respective cellular environments as compared to MG1655 GroES/EL. Isoelectric point and molecular weight data were generated using ExPASy Computer pI/Mw data tool. Gram positives (*E. faecium*, *S. aureus*) have overall fewer number of residues, lower isoelectric point, and are lacking C terminal GGM repeat compared to gram negative organisms (*K. pneumonia*, *A. baumannii*, *P. aeruginosa*, E. *faecium*, and *E. coli)*.

Individual ESKAPE pathogen pBAD *groESL* plasmids (Kan^R), MG1655 pBAD *groESL* plasmid (Kan^R), or empty vector (EV) (Kan^R) were transformed into LG6 (Cam^R) and plated onto chloramphenicol/kanamycin agar supplemented with agents as listed in (Fig. 3A). Arabinose induction within this system generates notable levels of GroESL from the plasmid. Conversely, native chromosomal GroESL is maintained at low levels due to the aforementioned *lac* promoter leak. Under these conditions, *K. pneumoniae*

(KP), *A. baumannii* (AB), *E. cloacae* (EC), and *E. coli* (Coli) *groESL* plasmid induction successfully complemented GroESL-deficient LG6. Despite producing soluble GroESL, *E. faecium* (EF) and *P. aeruginosa* (PA) were unable to rescue LG6. *S. aureus* (SA) GroESL also did not rescue LG6, but was noted to produce insoluble protein in this system (not shown). The empty vector was incapable of rescuing the model organism. This seems to have been caused by the absence of sufficient intracellular GroESL. LG6 not subjected to transformation could not proliferate on the chloramphenicol/kanamycin plates due to the absence of kanamycin resistance and insufficient GroESL production at the respective dilution (Fig. 3A). We carried out an identical experiment, supplementing agar plates with IPTG. Induction with IPTG promotes elevated levels of GroESL expression from the LG6 chromosome. Again, EF, SA, and PA were incapable of facilitating rescue despite GroESL expression from the LG6 chromosome, which otherwise would be expected to produce viable organism (Fig. 3B). To evaluate the possibility of producing alternate results from an experimental arrangement based upon gene dosage of both chromosomal and plasmid-borne *groESL* copies, organisms subjected to transformation were plated on antibiotic plates supplemented with arabinose in addition to IPTG. We were surprised to discover that EF, SA, and PA still could not rescue LG6 (Fig. 3C). Plasmid and chromosomal *groESL* transcriptional leakage were evaluated by glucose supplementation of agar plates. As evident in Fig.

3D, glucose suppression resulted in decreased colony number, but could not completely abrogate GroESL expression from either plasmid or chromosomal sources. Furthermore, the addition of IPTG and glucose to agar plates facilitated the rescue of KP, AB, EC, and *E. Coli* in addition to LG6 transformed with EV, but once again failed at wholly suppressing plasmid derived GroESL by a dominant negative effect as observed in EF, SA, and PA transformed LG6 (Fig. 3E) Uninduced pBAD-promoted *groESL* plasmids rescued LG6 without induction likely due to leak (Fig. 3F). Expression of native LG6 GroESL in the presence of plasmid-delivered EF, SA, or PA GroESL appears to be lethal to the organism and may be explained by previous work regarding assembly of nonfunctional mixed-multimeric complexes.[11,12] Amino acid identity and similarity were compared between ESKAPE pathogens and MG1655 for GroESL to explain the dominant negative observations (see supplementary Tables S2,S3). SA and EF had the lowest identity and similarity to MG1655 GroESL, however PA had greater identity/similarity compared to AB but did not facilitate rescue. This unexpected phenomenon could not be explained exclusively by examination of amino acid sequence alone.

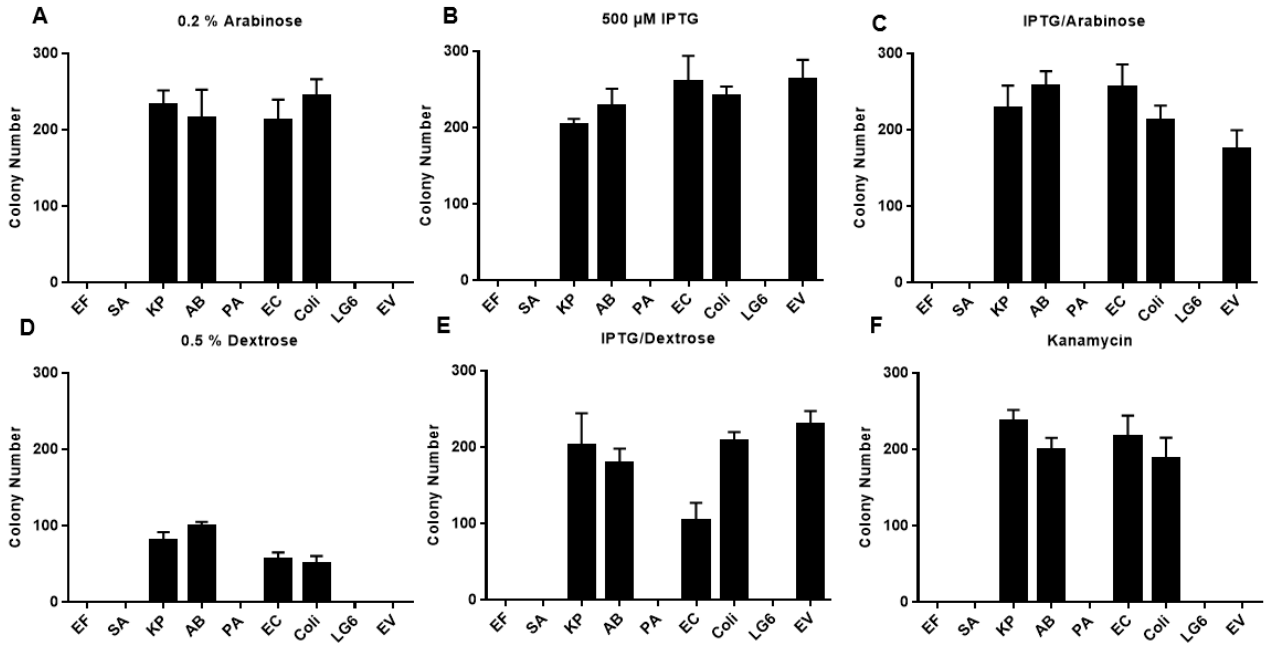

Figure 3. Among *K. pneumoniae* (KP), *A. baumannii* (AB), and *E. cloacae* (EC) Of ESKAPE pathogens, only KP, AB, and EC pBAD *groESL* (KmR) plasmids rescued LG6, the GroESL deficient *E. coli* strain. LG6 colony number from antibiotic selection plate reported after transformation with individual ESKAPE pBAD promoted *groESL* (KmR) plasmid, *E. coli* pBAD groESL (KmR) plasmid, or pBAD (KmR) empty vector. LG6 (CmR) did not grow on kanamycin infused plates. (A) 0.2% arabinose/kanamycin. (B) 500 µM IPTG/kanamycin. (C) 500 µM IPTG/0.2% arabinose/kanamycin. (D) 0.5% dextrose/kanamycin. (E) 500 µM IPTG/0.5% dextrose/kanamycin. (F) Kanamycin. The presented data represents at least three independent experiments and is reported as a mean with SD. *E. faecium* (EF), *S. aureus* (SA), *K. pneumoniae* (KP), *A. baumannii* (AB), P. aeruginosa (PA), *E. Cloacae* (EC), *E. Coli* (Coli), empty vector (EV).

Homology Modeling Reveals Structural Similarities Between the ESKAPE Pathogens and Alludes to Possible Structural Causes of a Dominant Negative Effect in the GroESL-deficient E.coli strain MG1655.

ESKAPE amino acid alignment with MG1655 GroEL monomer PDB 4pko.1.B, conducted within the PyMOL molecular visualization system, allowed us to observe the

conservation of similar structural features across several organisms (Fig. 4). Despite predicted structural retention among the ESKAPE pathogen GroEL and that of *E. coli*, amino acid substitutions were discovered in all three domains for each of the ESKAPE GroEL homology models (Fig. 4). In particular, there are significant structural alterations between *E. faecium*, *S. aureus*, *A. baumannii*, *P. aeruginosa* GroEL and that of *E. coli*, as highlighted by nonuniformity in amino acid identity throughout several regions comprising the proteins. These alterations are depicted here in two colors, purple when describing similar residues and red to distinguish those which are completely unique. The presence of distinctions in amino acid identity between the various structural aspects of the aforementioned pathogens and *E. coli* led us to believe that the incompatibility observed throughout our earlier experiments may be attributable to specific polypeptide domains within GroEL. Our persisting suspicions regarding the possible manifestation of a complementarity-inhibiting dominant negative effect resulting from hypofunctional GroEL mixed complexes during *E. Faecium, S. aureus, and P. aeruginosa* GroESL expression in LG6 (Fig. 3) added to our interest in performing a domain-specific investigation. Therefore, we elected to conduct a series of domain swapping experiments in hopes of identifying the domains of GroEL native to the ESKAPE pathogens responsible for the surprising dominant-negative aberrance.

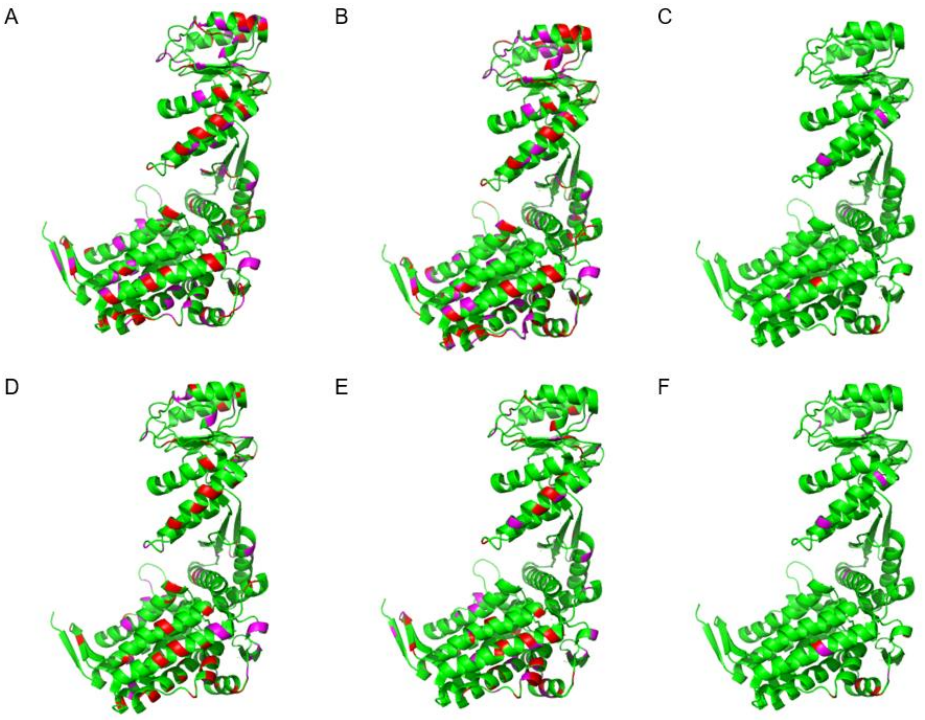

Figure 4. ESKAPE pathogen GroEL expresses similar and distinct residues in all three domains compared to *E. coli* 4pko.1.B. Identical residues in green, similar in purple, and distinct in red. (A) *E. faecium* (EF) and 4pko.1.B. (B) *S. aureus* (SA) and 4pko.1.B (C) *K. pneumoniae* (KP) and 4pko.1.B (D) *A. baumannii* (AB) and 4pko.1.B (E) P. aeruginosa (PA) and 4pko.1.B (F) , *E. cloacae* (EC) and 4pko.1.B. Protein models were generated in PyMOL.

We elected to conduct domain swaps using QuickStep cloning. The protein product of these plasmids was induced by arabinose in LG6 and complementation was measured by colony count. Chimeras comprised of *P. aeruginosa* intermediate and apical domain and an *E. coli* equatorial domain successfully rescued the GroESL deficient *E. coli* (Fig. 5). Likewise, chimeras constituted by *E. faecium* intermediate and *E. coli* apical and equatorial domains proved capable of rescuing the GroESL deficient organisms (Fig. 5). The functionality of the former chimeras was confirmed via an evaluation of polypeptide ATPase activity—a biochemical metric used to represent GroEL-mediated polypeptide refolding efficacy—which revealed wild-type

activity levels for *E. coli* and *P. aeruginosa* GroEL as well as notable activity for chimeras constituted by *P. aeruginosa* intermediate and apical and *E. coli* equatorial domains Fig. 6). Conversely, GroEL chimeras constituted by *P. aeruginosa* equatorial domains and *E. coli* intermediate and apical domains were unable to rescue the GroESL deficient bacteria (Fig. 6). This was also the case for the *E. faecium* intermediate and apical domain and *E. coli* equatorial domain bearing chimeras and equally true for chaperonins constituted by *E. faecium* equatorial domain and *E. coli* intermediate and apical domains (Fig. 6). As in the former cases, chaperonin rings comprised of *E. faecium* apical and *E. coli* equatorial and intermediate domains failed to rescue the GroESL deficient *E. Coli* strain LG6 (Fig. 5).

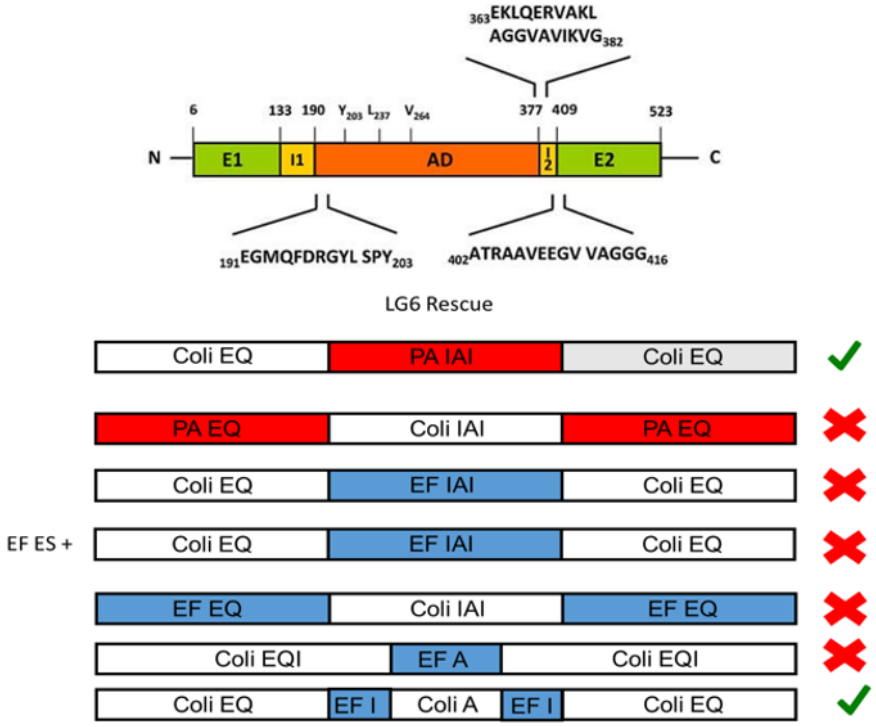

Figure 5. QuickStep-Cloning was used to generate GroEL domain swaps to evaluate organism rescue in GroESL deficient *E.* coli. E*. coli* domains (white) were paired with *P. aeruginosa* (red) or *E. faecium* (blue) to determine domain compatibility between organisms.

Collectively, these results suggest a lack of complementarity between the apical and intermediate domains of *E. faecium* and the equatorial domains of *E. coli*, this also being valid for *E. faecium* equatorial and *E. coli* intermediate and apical domains. However, this absence of complementarity does not necessarily prevent the expression of *E. faecium* / *E. coli* GroEL mixed complex over brief periods as we soon came to understand.

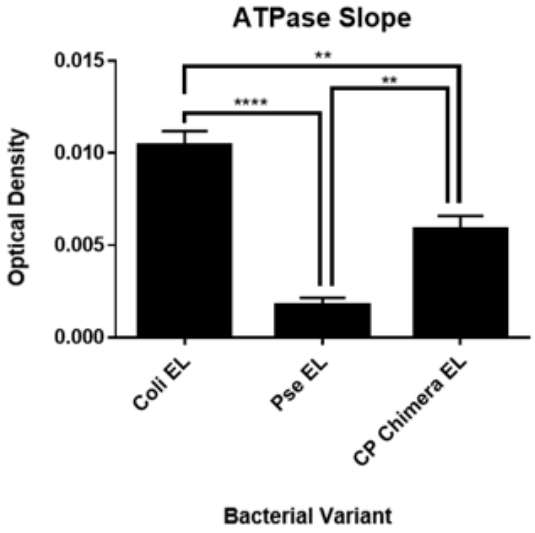

Figure 6. Although chimeric GroEL comprised of *P. aeruginosa* intermediate and apical and *E. coli* equatorial domains exhibits notable ATPase activity, it is not as fluent as that of *E. coli* alone.

Our approach to testing our GroEL mixed complex formation hypothesis was predicated significantly on previous work involving native mixed-ring assemblies conducted by Chapman et.al as well as earlier investigators. Mixed-ring composites, each defined by coexpression of *E. coli* GroEL △532/473C—(chaperonins bearing a cysteine mutation at position 473 for capture on a Thiopropyl sepharose column and removal of C terminal GGM repeat, allowing for distinct separation of this mutant from wild-type via SDS-PAGE)—and select ESKAPE GroEL were generated from distinct plasmids containing either *trc* or *ara* promoters (Fig .7).[11] Dissimilar relative

concentrations of IPTG and arabinose were used to induce the expression from each GroEL plasmid (Fig. 7).[11]

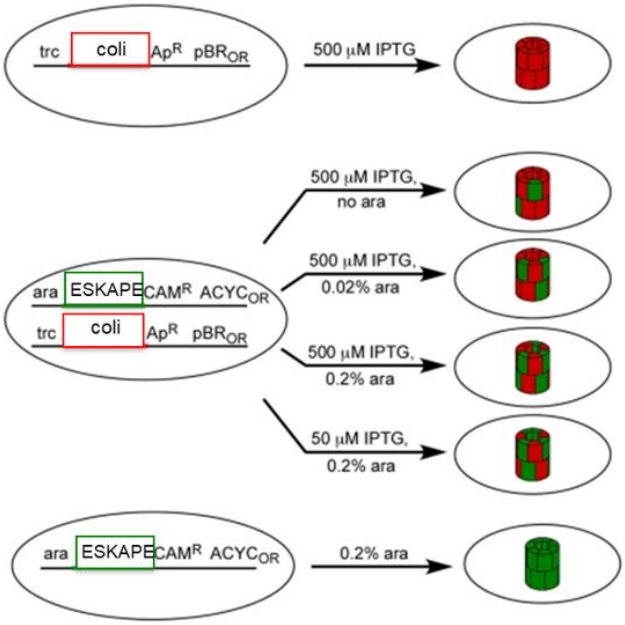

Figure 7. Schematic of mixed complex formation involving GroEL coexpression within BL21. Varying concentrations of IPTG and arabinose are used for induction

Mixed complex expression was achieved and confirmed by way of *E. coli* △532/D473C and nonnative GroEL coexpression followed by purification using an FFQ anion column and final capture using Thiopropyl sepharose followed by DTT elution of the desired protein. Results were obtained by SDS-PAGE analysis (Fig. 8). *E. faecium*/△532/D473C EL mixed complex in *E. coli* was captured with the use of an identical method and observed by SDS-PAGE (Fig. 8). The successful expression of the *P. aeruginosa*/△532/D473C EL mixed complex was also visualized (Fig 8).

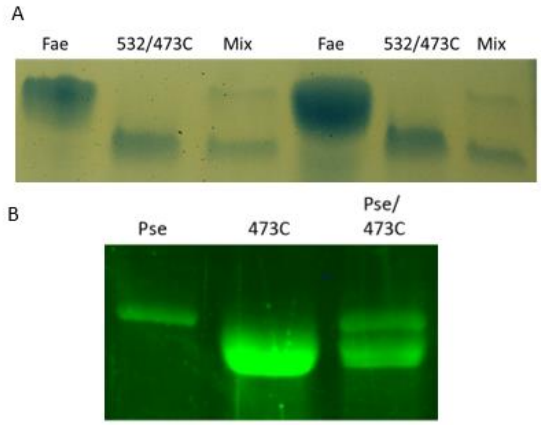

Figure 8. (A) *E. coli* △532/D473C capture and *E. faecium*/△532/473C EL expression in *E. coli* reveals GroEL mixed complex on SDS-PAGE. **(B)** *E. coli* △532/D473C capture and *P. aeruginosa*/△532/473C EL expression in *E. coli* GroEL mixed complex on SDS-PAGE.

As in the chimerization experiments discussed previously, a study of ATPase activity was implemented in the evaluation of each conclusively expressed mixed complex. Despite robust expression of *E. faecium*/△532/473C EL, little to no ATPase activity was associated with the mixed complex (Fig. 9.). This was in contrast to Faecium EL and 473C EL which both showed relatively significant activity (Fig. 9). Similarly, The *P. aeruginosa*/△532/473C EL mixed complex in *E. coli* showed diminished ATPase activity alone or in combination with GroES compared to individually expressed counterparts.

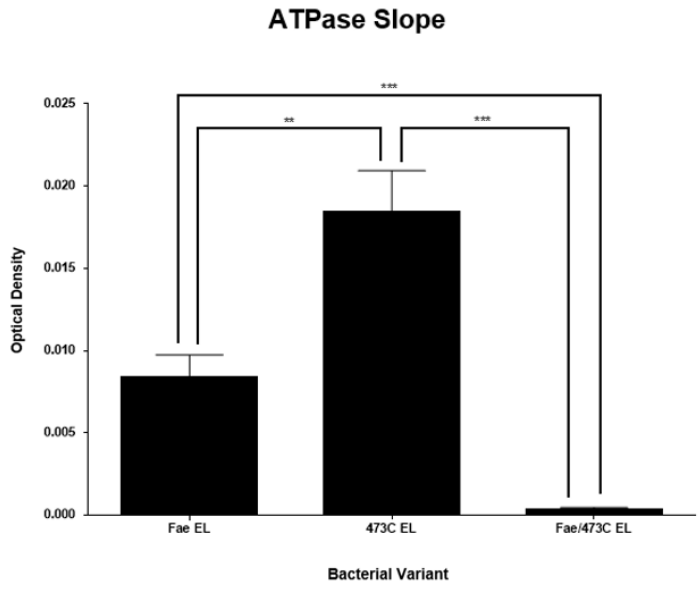

Figure 9. *E. faecium*/△532/473C EL mixed complex exhibits diminished ATPase activity and E. faecium or △532/D473C alone.

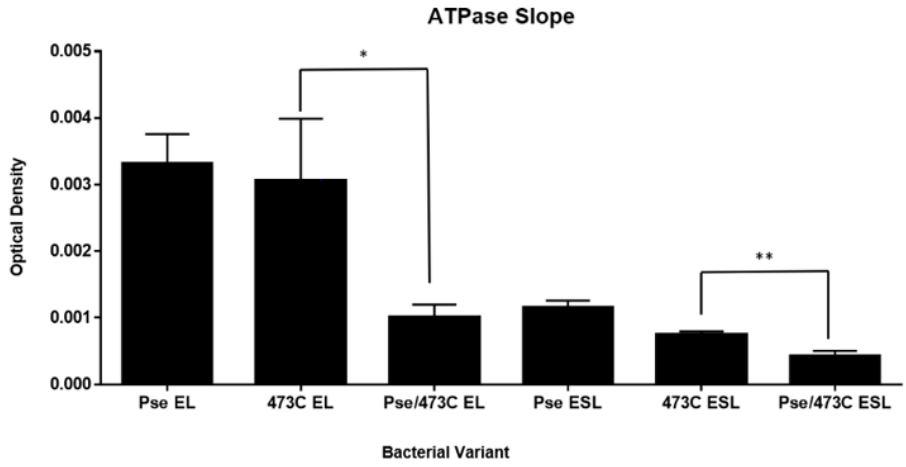

Figure 10. *P. aeruginosa*/△532/473C EL demonstrates impaired ATPase activity alone or in combination with GroES compared to individually expressed GroEL.

P. aeruginosa **Rescues** ***groEL*****-null** ***E. coli*** **Strain AI90.**

We elected to use the AI90 strain to further support our hypothesis that native and nonnative GroEL incompatibility could be responsible for the dominant-negative phenotype evident in GroEL-deficient LG6 in the presence of EF, SA, and PA.[13] The AI90 strain retains wild type *groES,* while kanamycin replaces *groEL* on the chromosome within the *groESL* operon. AI90 was maintained by *E. coli* GroEL produced from a pACYC plasmid (Cam^R) containing *E. coli groESL* and *sacB*. In the presence of sucrose, the *sacB* protein product generates levans which exhibit toxicity towards gram-negative bacteria, allowing for selection against this plasmid. pACYC-pBAD ESKAPE *groESL* and *E. coli groESL* plasmids, as well as empty vector, were individually transformed into AI90 and plated on agar supplemented with ampicillin,

sucrose, and arabinose (Fig. 11A). This system allowed for selection of transformants that could shuffle out the *E. coli* groESL/sacB plasmid while retaining the newly introduced ESKAPE *groESL* plasmid lacking the *sacB* gene. Colonies arising from this process rescue the organism by supplying a functional GroESL system capable of complementing *E. coli* in the presence of *E. coli* GroES expressed from the chromosome. In addition to *K. pneumoniae* (KP), *A. baumannii* (AB), *E. cloacae* (EC), and *E. coli* (Coli), all of which rescued GroESL deficient LG6, we discovered that *P. aeruginosa* (PA) was capable of rescuing *groEL*-null AI90 (Fig. 11B). To ensure that *groESL-sacB* plasmids were not retained in these viable rescues, plasmid isolation was conducted from these colonies and ran on an agarose gel. All of the gram-negative ESKAPE pathogen *groESL* (KP, AB, EC, and PA) along with E. coli *groESL* plasmids failed to retain *groESL-sacB* plasmid (Fig. 11C). The ability of PA *groESL* to rescue a *groEL*-null, but not GroEL-deficient *E. coli* strain alludes to incompatibility among their GroEL chaperones. Incorporation of *E. coli* and PA GroEL into the same multimeric unit produces a hypofunctional or nonfunctional chaperonin unable to support bacterial survival, even when organisms are grown in optimal growth conditions as discussed earlier.

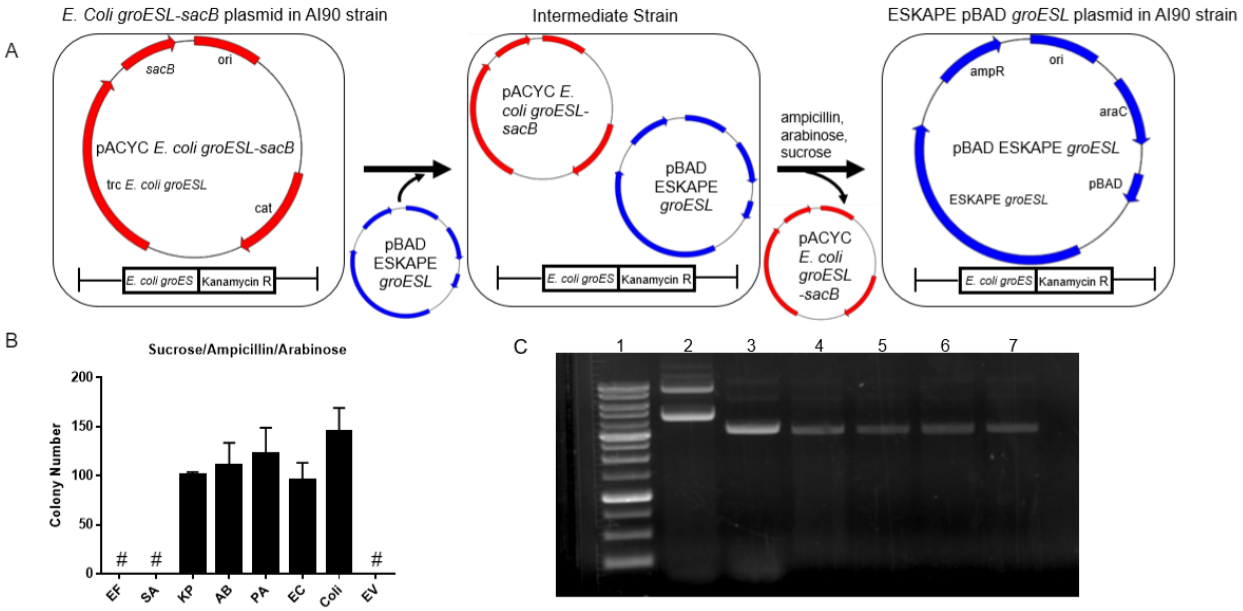

Figure 11. All gram negative ESKAPE pathogens rescued *groEL* deficient AI90 strain after *sacB* pACYC *groEL* (CmR) plasmid shuffle with pBAD ESKAPE groESL plasmid.(A) Scheme of ESKAPE *groESL* plasmid shuffle into *E. coli groEL*-null background AI90 strain. (B) AI90 colony number from 5% sucrose/0.2% arabinose/ampicillin selection plate reported after transformation with individual ESKAPE pBAD *groESL* (AmpR) plasmid, *E. coli* pBAD *groESL* (AmpR) plasmid, or pBAD (AmpR) empty vector. # colonies were visualized on these plates but retained mutant *sacB groEL* plasmid. Represented by three independent experiments and reported as mean with SD.(C) All gram negative ESKAPE pathogens rescued *groEL* deficient AI90 after *sacB* pACYC *groEL* (CmR) plasmid shuffle. Plasmids from surviving colonies after shuffle were isolated and ran on 0.5% DNA gel. Lane 1, DNA ladder; lane 2, *sacB* pACYC *groEL* plasmid; lane 3, E. coli pBAD promoted *groESL*; lane 4, EC pBAD *groESL*; lane 5, AB pBAD *groESL*; lane 6, KP pBAD *groESL* plasmid; lane 7, PA pBAD *groESL* plasmid.

***E. faecium* and all gram negative ESKAPE pathogen *groESL*, but not *S. aureus* *groESL* Knock-in/Knock-out Rescues MG1655.**

To investigate the ability of ESKAPE GroESL to complement an *E. coli* strain devoid of wild-type GroESL expression, the lambda Red recombinase system was employed to

individually knock-in ESKAPE *groESL* into the MG1655 *groESL* operon.[14] Due to high homology between the gram-negative ESKAPE pathogens (KP, AB, PA, EC) and MG1655, ESKAPE knock-ins were generated from the first successful complete knock-in, *E. faecium* (Fig. 12). This process involved constructing a PCR-generated insertion cassette which contained ESKAPE *groESL,* an antibiotic resistance marker chloramphenicol acetyl transferase (CAT), and flippase recognition target (FRT) sites for future removal of antibiotic resistance, all flanked by a 50 base pair overhangs homologous to regions up/down stream of the *groESL* operon in MG1655. The insertion cassette was transformed into MG1655 in the presence of lambda Red recombinase plasmid pKD46 and plated on agar supplemented with antibiotic for selection of this knock-out/knock-in construct. Colonies arising from this process were confirmed to contain the correct insert by PCR and DNA sequencing (Fig. 12).*E. faecium* knock-in viability in this system suggests that *E. coli* GroES and perhaps GroEL are not compatible in the presence of this nonnative chaperonin. Of *S. aureus*, only a partial knock-in could be generated (C-terminus only) and thus was not further studied (Fig. 12). These data may point to deficiency in *S. aureus* GroESL assembly within the *E. coli* system. Therefore, intracellular factors external to the chaperonin itself may be worthy of consideration in future studies.

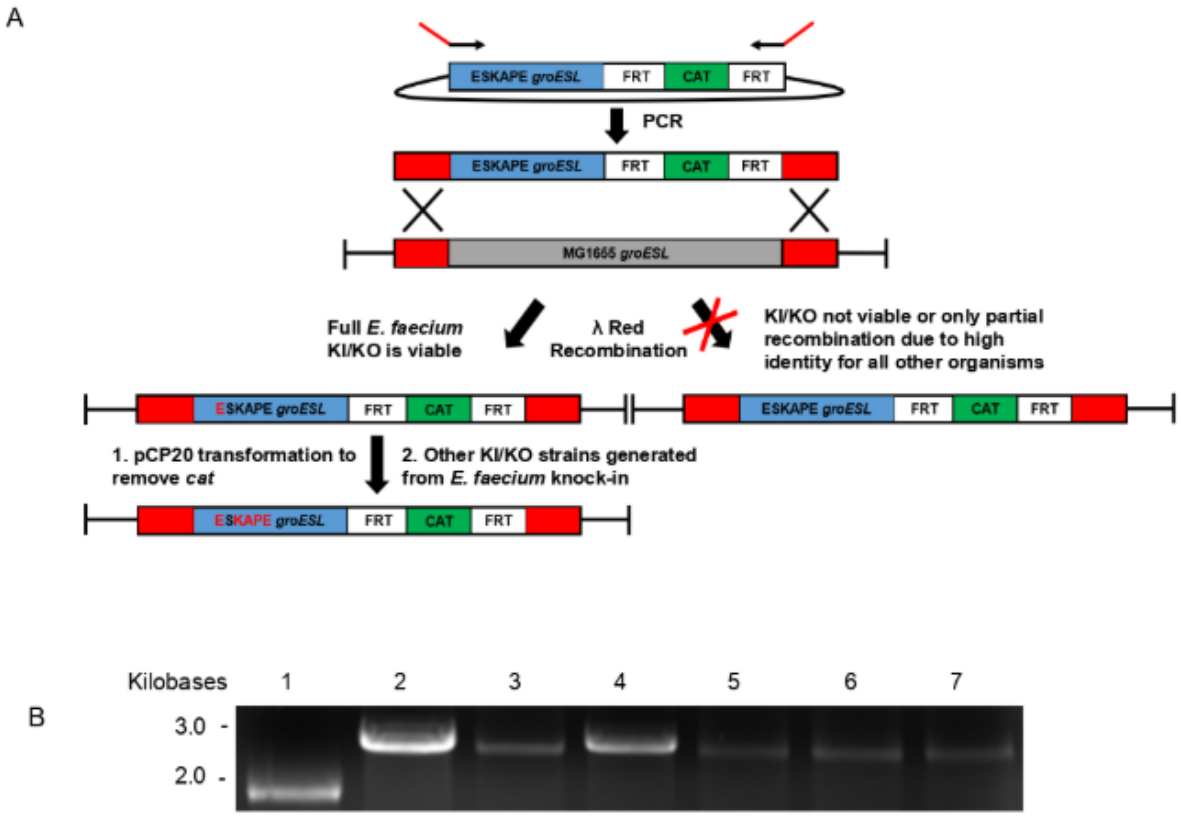

Figure 12. ESKAPE *groESL* knock-ins generated by utilizing λ red recombinase system in MG1655 strain. (A) Due to high sequence identity between ESKAPE pathogens and *E. coli groESL,* only MG*ΔgroESL*::EF *groESL*(Cam^R) could be obtained from knock-in (lower *groESL* sequence homology compared to gram negative pathogens). From this knock-in, KP, AB, PA, and EC *groESL* knock-ins were generated. Full SA *groESL* knock-in could not be obtained. (B) PCR products for MG1655 and knock-ins for all ESKAPE pathogens using primers flanking *groESL* gene visualized on agarose gel. Lane 1, MG1655 WT *groESL*; lane 2, MG*ΔgroESL*::EF *groESL*(Cam^R); lane 3, MG*ΔgroESL*::SA *groESL*(Cam^R) partial knock-in; lane 4, MG*ΔgroESL*::KP *groESL*(Cam^R); lane 5, MG*ΔgroESL*::AB *groESL*(Cam^R); lane 6, MG*ΔgroESL*::PA *groESL*(Cam^R); lane 7, MG*ΔgroESL*::EC *groESL*(Cam^R).

ESKAPE *groESL* Knock-ins Have Temperature-dependent Phenotypic Changes, but Similar Growth Kinetics to Wild-type MG1655.

Proteins used in cell division, such as FtsZ, have been identified as clients of GroEL.

GroEL has been shown to localize at cell division sites and depletion of this chaperonin in *E. coli* produces an elongated phenotype.[16,4] Knock-ins were grown to mid-log phase at 24 or 42 °C and imaged to determine if MG1655 with nonnative GroESL was subject to defects in binary fission. Cultures grown at heat shock temperatures (42 °C) promote elevated expression of chromosomal GroESL than at 24 °C.[22] *E. faecium*, *K. pneumoniae*, and *E. cloacae groESL* knock-ins demonstrated phenotypic elongation at 24, but not 42 °C (Fig. 13). Conversely, *P. aeruginosa* exhibited changes in cell morphology at heat shock temperature, but not at room temperature. MG1655 and *A. baumannii* knocks-ins did not display altered phenotype at either temperature.

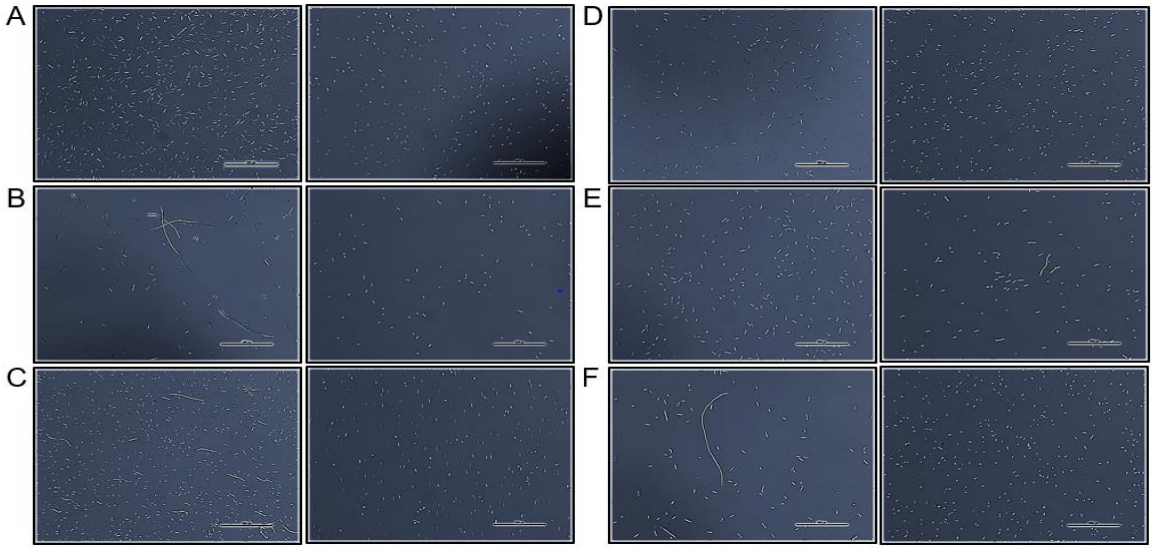

Figure 13. MGΔgroESL::ESKAPE groESL (CmR) show elongated phenotype at various temperatures compared to parent strain, MG1655, between 24 and 42 °C. 40X images captured for each strain after growth to mid-log phase in LB media without antibiotic at stated temperatures. (A) MG1655 24 °C (Left) and MG1655 42 °C (Right). (B) MGΔgroESL::EF groESL 24 °C (Left) and MGΔgroESL::EF groESL 42 °C (Right). (C) MGΔgroESL::KP groESL 24 °C (Left) and MGΔgroESL::KP groESL 42 °C (Right). (D)

MGΔgroESL::AB groESL 24 °C (Left) and MGΔgroESL::AB groESL 42 °C (Right). (E) MGΔgroESL::PA groESL 24 °C (Left) and MGΔgroESL::PA groESL 42 °C (Right). (F) MGΔgroESL::EC groESL 24 °C (Left) and MGΔgroESL::EC groESL 42 °C (Right). Scale represents 80.5 µm. Scale added to A (left image).

Surprisingly, a similar growth rate was observed at heat shock and non-heat shock temperatures between ESKAPE knock-ins and wild-type MG1655 (Fig. 14). This suggests that replacement of wild-type GroESL with ESKAPE GroESL does not alter organism laboratory fitness with exception to chaperonin derived from *S. aureus,* which had shown to be noncomplementary in a multitude of rescue systems.

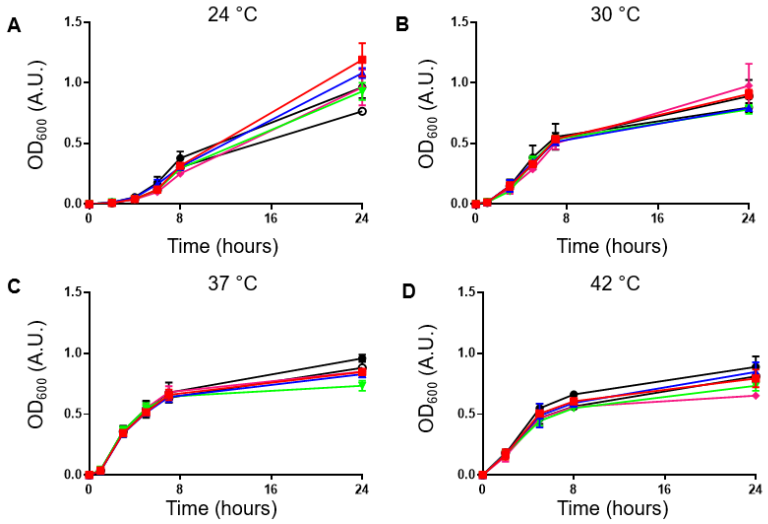

Figure 14. MG1655*ΔgroESL*::ESKAPE *groESL* (CmR) show similar growth kinetics compared to parent strain, MG1655, between 24 and 42 °C. In three independent experiments and reported as mean with SD, growth in LB media without antibiotic at stated temperature was measured by OD_{600} over time to determine growth rate of each individual strain. (A) Growth at 24 °C. (B) Growth at 30 °C. (C) Growth at 37 °C. (D) Growth at 42 °C. Black, MG1655, red, MG1655*ΔgroESL*::EF *groESL* (CmR), blue, MG*ΔgroESL*::AB *groESL* (CmR), green, MG*ΔgroESL*::KP *groESL* (CmR), pink, MG*ΔgroESL*::PA *groESL* (CmR), open/white, MG*ΔgroESL*::EC *groESL* (CmR).

DISCUSSION

This study builds upon previous works where subunit mixing techniques—specifically

those used to exchange wild-type subunits for wild-type variants—were employed to evaluate the complementation and tolerability of ESKAPE GroEL to E. coli GroEL.[15,4] Functionality and complementation of ESKAPE GroEL was determined in *E. coli* using a stepwise approach starting with GroESL deficient *E. coli* strain, LG6. Quantified by members of the Lund Group, a significant depletion of GroEL in *E. coli* results in nonviable organism.[16] Due to leak from *lac*-regulated *groESL*, GroESL produced at working organism dilutions is unable to support colony growth on agar in the LG6 cell line. Coexpression of nonnative GroESL within this system allows for the possibility of incorporation of wild-type and ESKAPE GroEL subunits into the GroEL ring. Facilitation and disassembly are driven by noncovalent forces, dictated by equatorial domain interactions.[17] Incompatibilities between native and nonnative GroEL equatorial domains may, in some cases, prevent the formation of functional homotetradecamer or may result in formation of lower states of nonfunctional GroEL. Furthermore, differences in ATP utilization between ESKAPE and wild-type GroEL could lead to perturbation of ATP hydrolysis and loss of coordinated allosteric changes in the GroEL folding cycle. Protein allostery could also be affected by significant differences in intermediate or apical domains.[18,19]

Gained from the LG6 experiment was the observation that half of the GroESL

chaperonins within the ESKAPE family, when expressed in the presence of wild-type, could not rescue the organism, and ultimately produced a dominant-negative phenotype. *P. aeruginosa* exhibited significant similarity when compared to *E. coli* GroESL, but the variants did not complement in this experimental setup. Moving to the *groEL*-null AI90 strain, *P. aeruginosa* complemented in this system, suggesting that *P. aeruginosa* GroEL could rescue *E. coli*, but not in the presence of *E. coli* GroEL. Domain swapping experiments partially reinforced this conclusion as chimeras comprised of *P. aeruginosa* equatorial domains and *E. coli* intermediate and apical domains were unable to facilitate rescue in *E. coli*, suggesting domain-specific causes of the dominant negative effect. However, chimeras constituted by *P. aeruginosa* intermediate and apical and *E. coli* equatorial domains proved capable of rescuing *E. coli*. This observation offers some opposition to the idea that *P. auruginosa* cannot rescue *E. coli* in the presence of *E. coli* GroEL. In fact, it seems to suggest that the dominant negative effect observed in LG6 during *P. auruginosa* and *E. coli* coexpression may be associated with the equatorial domain of *P. auruginosa* GroEL in some capacity. This suspicion is further supported by Fig. 4E which predicts the presence of a significant number of amino acid residues in the equatorial domain of *P. auruginosa* GroEL distinct from those comprising the same region of the *E. coli*

homologue. Therefore, it may be possible that the presence of the *P. aeruginosa* equatorial domain within the *P. auruginosa* equatorial and *E. coli* intermediate and apical domain-comprised chimera may play a part in preventing the chaperonin from refolding polypeptides into their proper structures. This is a troublesome event within the cell, as misfolded polypeptides lose some or all of their ability to perform important intracellular functions causing the organisms within which they are expressed to quickly expire.

Successful expression of *P. auruginosa*/*E. coli* during our mixed complex experiments (Fig. 8B) suggested that properly folded chimeric and/or mixed homotetradecameric chaperonins do indeed form but are significantly less active within the cell than their wild-type counterparts. Therefore, we suspect that the *P. auruginosa* equatorial domain of the *P.* auruginosa/*E. coli* chimeric and mixed composites likely participates in allosteric events associated with chaperonin-mediated polypeptide refolding. This proposition offers support for the idea that the dominant negative effect observed throughout our LG6 experiment is linked to the formation of mixed ring chaperonins, whose altered structures cause them to become more sensitive to inhibitory allosteric events and reduce their chaperoning ability. The inability of mixed-ring chaperonins to fold nascent and/or misfolded polypeptides would impair cellular

viability due to an absence of properly folded intracellular proteins critical for the proper execution of various intracellular tasks. Unlike the *P. auruginosa* equatorial domain-bearing chimera, GroEL comprised of *P. aeruginosa* intermediate and apical and *E. coli* equatorial domains exhibited notable, albeit reduced—when compared to wild-type *E. coli*—GroEL ATPase activity (Fig. 5). This reduction in ATPase activity indicated that chimeras comprised of *E. coli* equatorial and *P. auruginosa* intermediate and apical domains were not as fluent at folding polypeptides as the corresponding chaperonin in *E coli* on its own despite their ability to keep bacteria alive. As discussed above, a reduction in ability to hydrolyze ATP may be in rooted modifications associated with chaperonin allostery.

The *P. auruginosa* GroEL model depicted in Fig. 4E offers insight into the possible structural basis potentially responsible for changes in chimeric chaperonin sensitivity to allosteric inhibition, as it contains several short stretches of amino acid residues within its apical and intermediate domains distinct from those comprising the *E. coli* homologue. There is a significantly greater number of amino acid differences between the equatorial domains of *P. auruginosa* and *E. coli* compared to the apical and intermediate domains of the respective chaperonins. The lesser number of distinctions between the primary structures comprising the *P. auruginosa* apical and intermediate

domains and the corresponding substructures in *E. coli* may be why the relevant chimeric GroEL is capable of some ATPase-dependent polypeptide refolding activity. Greater similarity of the aforementioned domains in *P. auruginosa* to corresponding structures in *E. coli* may allow for the assembly of a chaperonin that exhibits reduced rather than completely absent ability to refold polypeptides. If allosteric inhibition does play a role in chaperonin-mediated polypeptide refolding efficiency, the relative similarity of *P. auruginosa* GroEL apical and intermediate domain structure to that of corresponding substructures in *E. coli* may facilitate only a moderate loss of chaperonin-mediated ATPase activity representative of chaperoning action.

In the case of chimeras partially comprised by *P. auruginosa* equatorial domains, the significant number of distinctions between the primary structures comprising these and the corresponding substructures in *E. coli* may be far too disruptive to the polypeptide refolding ability of chimeric GroEL. The loss of folding ability may originate from structural impingements to folding-cycle rearrangements within chaperonins whose *P. auruginosa* equatorial domains are incapable of proper interaction with the apical and intermediate domains of *E. coli*. The chaperonin's inability to perform certain folding cycle-related rotations and rearrangements may be due to steric hinderance between the amino acids of the equatorial and intermediate domains of the relevant chimeras.

Ultimately, the nonfunctional quaternary form of the chaperonin, resulting from amino-acid mediated disruption of folding cycle-related structural rearrangements, would prevent it from conducting equatorial domain-mediated ATP-hydrolysis.

We determined that *E. faecium* did not complement in the GroESL-deficient or *groEL*-null systems. However, simultaneous knock-out of MG1655 *groESL* and knock-in of *E. faecium groESL* produced viable organismal colonies. From this observation, it may be reasonable to conclude that the previous lack of organism rescue may be attributed to impairment of chaperonin function as a result of *E. faecium/E. coli* GroEL ring mixing. Furthermore, *E. faecium* GroEL and/or *E. faecium/E. coli* oligomeric ring formation may result in disruption of interaction with *E. coli* GroES or loss of GroES release after folding cycle, resulting in the loss of refolding function. Domain swapping experiments revealed that compatibility between *E. faecium* and *E. coli* GroEL, although extremely limited, does exist. Indeed, *E. faecium* intermediate and *E. coli* apical and equatorial domain-comprised chimeras proved capable of rescuing GroESL deficient organisms. However, chimeras consisting of *E. faecium* intermediate and apical and *E. coli* equatorial domains were unable to rescue GroESL deficient bacteria. This was also true for chimeras constituted by *E. faecium* equatorial and *E. coli* intermediate and apical domains (Fig. 8A.). Chimeras comprised by *E. faecium* apical and *E. coli*

equatorial and intermediate domains also failed to rescue the GroESL deficient *E. Coli* strain. These results suggest that the viability of *E. faecium*/*E. coli* GroEL chimeras is absolutely dependent on the simultaneous presence of apical and equatorial *E. coli* domains within the chaperonin. This revelation alludes to the idea that *E. faecium* GroEL and/or *E. faecium/E. coli* oligomeric rings either prevent chaperonin interaction with *E. coli* GroES or promote the retention of the molecular lid at the apical domain of GroEL after the completion of the polypeptide refolding cycle. Support for this proposition is offered by the structure of the *E. faecium* homology model depicted in Figure 4A (and further supported in supplementary tables 1 and 2), which along with *S. aureus* and *A. baumannii* exhibits some of the highest differences in amino acid sequence (lowest similarity and identity) among the ESKAPE pathogens from that of *E. coli*. As with the equatorial domains of *P. auruginosa* discussed earlier, the multitude of distinctions in amino acids between *E. faecium* GroEL and *E. coli* GroEL, while non-inhibitory to homotetradecamer formation, are involved in the generation of inactive quaternary structures unless the equatorial and apical domains of the latter chaperonin are present within the chimera. Similarly to *P. aeruginosa and E. coli* GroEL, differences in amino acid sequences between the various *E. faecium* and *E. coli* GroEL domains likely cause reductions in chaperonin-mediated hydrolysis of ATP by imparting

modifications to the allosteric mechanisms associated with GroEL as discussed earlier. Furthermore, the presence of the *E. faecium* apical domain in place of the corresponding *E. coli* substructure may prevent the binding of GroES to the chimeric GroEL. Conversely, it is possible that these alterations allow GroES binding, but the structural rearrangement of the chimeric GroESL complex during the folding cycle may lock GroES into a continuous interaction with the *E. faecium* apical domain of the *E. faecium/E. coli* GroEL chimera. This in turn would prevent the release of folded polypeptides into the cytosol, rendering them unable to participate in intercellular events critical to cell survival. Therefore, we postulate that the general absence of complementarity between *E. faecium* and *E. coli* GroEL occurs as a result of significant differences in amino acid sequence throughout the physical constitution of these chaperonins.

Mixed complex experiments revealed that although *E. faecium*/△532/473C EL mixed-ring assemblies can be successfully generated in *E. coli*, they are hypofunctional in comparison to wild-type chaperonin variants. While robust expression of *E. faecium*/△532/473C EL was achieved (Fig. 8A), the ATPase activity attributed to it was miniscule (Fig. 9). These results suggest that although the mixed complex was successfully translated by the ribosomal machinery of *E. coli* folded properly, and

assembled homotetradecamer, it was incapable of efficient polypeptide refolding. We suspect that differences between the amino acid sequences comprising the various domains of *E. faecium* and *E. coli*, likely causes the arrangement of *E. faecium*/△532/473C EL mixed complexes into quaternary structures incapable of efficiently refolding other polypeptides due to allosteric mechanisms similar to those discussed earlier. This seems to be the case for the *P. aeruginosa*/△532/473C EL mixed complex in *E. coli*, which expressed rather well (Fig. 8B) yet showed minimal ability to hydrolyze ATP when compared to *P. auruginosa* EL and △532/473C EL (Fig. 10). As suspected in the domain swapping experiments and with *E. faecium*/△532/473C EL, mixed complexes involving *P. auruginosa* and *E. coli* exhibit significant differences in amino acid sequences throughout their various domains. Additionally, differences in amino acid sequences between the constituents of mixed complexes may prevent proper GroES interaction with GroEL as ATPase activity representative of these events observed in △532/473C ESL and *Pse*/△532/473C ESL is rather low (Fig. 10.). As in the case of the domain swaps, GroES may be unable to bind to GroEL and encapsulate polypeptides within the polypeptide-containing cavity. This in turn may prevent the onset of substrate induced, GroEL equatorial domain-mediated ATP hydrolysis. It is possible that GroES binding to GroEL is necessary for the initiation of apical, intermediate, and

equatorial domain rearrangements within the mixed-complex. Rearrangements of this nature may be necessary for the initiation of equatorial-domain mediated ATPase activity. Alternatively, it may be that GroES does bind to GroEL mixed complexes but does so in an incorrect fashion. Due to amino acid distinctions throughout the apical, intermediate, and equatorial domains of the mixed complex, GroES may become incapable of detachment once it has enclosed the polypeptide containing-cavity, thereby trapping polypeptides inside of the chaperonin and structurally hindering the initiation of equatorial-domain mediated hydrolysis of ATP. In summary, chimeric and mixed complex hypofunctionality, as evidenced by reductions in ATPase activity compared to wild-type organisms, seems to be structural in origin.

MATERIALS AND METHODS

Plasmids and Strains

GroES and GroEL DNA sequences were generated using genomic DNA obtained from *E. faecium* ATCC51559, *S. aureus* ATCC25923, *K. pneumoniae* ATCC700603, *A. baumannii* ATCC19606, *P. aeruginosa* ATCC47085, *E. cloacae* ATCC13047, and *E. coli* MG1655 bacterial strains (Table. 1). Structural similarity, identity, isoelectric points and molecular weight of GroEL and GroES native to each aforementioned organism were predicted using the ExPASy Computer pl/Mw data tool (Table. 1). Chimeric

GroEL was generated from previously described E. coli GroEL or ESKAPE GroEL pSpeed plasmids using PCR based QuickStep cloning. *E. coli* GroESL and ESKAPE GroESL were cloned into pSpeed plasmids using PIPE cloning.

DNA Recombineering

λ-red recombination, a straightforward and efficient gene disruption technique, was used as a means to introduce ESKAPE pathogen GroESL operons into *E. coli*. First, a DNA construct constituted by ESKAPE groESL and FRT (FLP) recognition target sites flanking a chloramphenicol resistance gene was assembled. Next, PCR amplification of the FRT-flanked resistance gene (CAT) was performed. The primers flanking the downstream FRT site and ESKAPE GroESL were sequentially homologous to the terminal regions of the MG1655 *groE* operon. Using λ-red recombination, an insertion cassette bearing a selected ESKAPE GroESL gene was delivered into an MG1655 *E. Coli* strain by electroporation using a Bio-Rad instrument with 0.2 cm cuvettes.

As discussed throughout the results section of this work, the high degree of sequence identity between *K. pneumoniae, A. baumannii, P. aeruginosa, E. cloacae* and MG1655 GroESL prevented the successful knock-in of the respective constructs into the host organism. Therefore, *E. faecium* recombination products were used as templates for insertion of GroESL sequences attributed to *K. pneumoniae, A. baumannii, P. aeruginosa,* and *E. cloacae*. Inability to obtain a viable *S. aureus* knock-in

product through recombination using an insertion cassette targeting *groE* operon of MG1655 wild-type or *E. faecium* knock-in strains was not further addressed. To confirm that recombination was successful, PCR products for MG1655 and knock-ins for all ESKAPE pathogens using primers flanking the *groESL* gene were examined on a standard agarose DNA gel. pCP20 transformation was utilized to excise CAT from the DNA of all organisms receptive to recombination.

Bacterial Culturing and Microscopy

pBAD promoted pSpeed plasmids (Kan^R) were used to clone in *groESL* endogenous to *E. faecium*, *S. aureus*, *K. pneumoniae*, *A. baumannii*, *P. aeruginosa*, and *E. cloacae* were transformed individually into LG6 (Cam^R) using heat shock or electroporation. Bacteria residing in agarose-supplemented and agarose free media were subjected to induction by varying concentrations of nutrients mixed with antibiotic including 0.2% arabinose/kanamycin, 500 µM IPTG/kanamycin, 500 µM IPTG/0.2% arabinose/kanamycin, 0.5% dextrose/kanamycin, (E) 500 µM IPTG/0.5% dextrose/kanamycin, and (F) Kanamycin only. IPTG was used to promote elevated levels of GroESL expression from the LG6 chromosome. During GroESL overexpression of both chromosomal and plasmid-borne *groESL* copies, transformant organisms were plated on antibiotic plates supplemented with varying concentrations of arabinose and IPTG. Additionally, Glucose-mediated suppression was implemented in

studies of organismal suppression.

Knock-in *E.coli* were incubated at either 24°C, 30°C, 37°C, or 42°. Samples of the bacteria/tryptone-based media mixture were periodically collected with a pipette and introduced into a spectrophotometer. Optical density readings were conducted and bacterial capacity for light absorbance correlated to organismal growth at a wavelength of 600 nm. Additionally, samples were taken within mid-log phase of growth and bacteria were stained and visualized through a *Nikon Eclipse 50i* microscope at 40x magnification (Figure 11.).

Protein Purification, Expression and Mixed Complex Formation

Protein expression in BL21(DE3) cells was initiated after transformation with the plasmid of interest. Varying concentrations of arabinose or IPTG were used to induce protein expression in 2L of LB media in baffled flasks when OD reached 0.6 at 37°C for 1 to 4 hours. Next bacteria were subjected to centrifugation at 7000 RCF for 7 minutes. Bacterial pellet was lysed with 50 mM Tris (pH 7.4) and 1 mM PMSF. The suspension was disrupted by microfluidizer induced stress. Cell lysate was subjected to 2200 RCF for 45 minutes. Expression of protein of interest was verified by SDS page analysis from the centrifugated supernatant. Protein of interest was separated by anion exchange using FFQ resin with NaCl gradient from 0 to 0.5 M. D473C *E. coli*. GroEL was

incubated with Thiopropyl sepharose resin and a low concentration DTT wash was performed to disrupt nonspecific interaction. A higher concentration of DTT was used to elute protein of interest. Proteins residing within DTT eluted fractions were visualized by SDS page. Mixed-ring composites of 532△/473C *E. coli* GroEL subunits and select ESKAPE GroEL were produced using distinct plasmids containing either *trc* or *ara* promoters. Relative concentrations of IPTG and arabinose were used to induce the chimeric GroEL complexes.

ATPase Assay

A colorimetric malachite green assay involving inorganic phosphate was used to measure GroEL/GroESL-mediated ATP hydrolysis. 1 μM chaperonin in 50 mM Tris (pH 7.4), 50 mM KCl, 10, mM, and 1 mM DTT were used in the execution of the reaction.[4] The subsequent incubation of the mixture was performed at 23°C for 5 minutes. 50 μL aliquots were withdrawn at distinct points in time. The hydrolysis reaction was quenched by the introduction of the reactive solution into 800 μL of 0.034% (weight/volume) malachite green and 1.04% (weight/volume) ammonium molybdate in 1 μM HCl.[4] 100 μL of 34% (weight/volume) sodium citrate was introduced into the reaction mixture 1 minute after the quench. 5-30 minutes were permitted to expire before a sample of the reaction mixture was introduced into a spectrophotometer and optical density was measured at 660 nm. Absorbance was converted to nanomoles or micromoles of

phosphate using a phosphate-based standard curve in reaction buffer.[4]

Modeling

ESKAPE pathogen GroEL models were generated using the PyMOL open source molecular visualization system. The amino acid sequence of *E. coli* GroEL was referenced by the modeling program throughout the generation of corresponding ESKAPE pathogen chaperonin models. Distinctions in residues between ESKAPE and *E. coli* GroEL were manually identified and highlighted.

FUTURE DIRECTIONS

In our upcoming studies of the relationship between ESKAPE pathogen and *E. coli* GroEL, we intend to test our theories regarding allosteric inhibition by investigating its role in the chaperonin's folding action. Understanding how ATP hydrolysis products affect the activity of domain swap and mixed complex chaperonins comprised of ESKAPE and *E. coli* GroEL, will allow us to better interpret why *P. auruginosa*/*E. coli* GroEL and *E. faecium*/*E. coli* GroEL exhibit reductions in polypeptide refolding function despite their robust expression in bacteria. Furthermore, we intend to launch a separate investigation around *S. aureus* GroEL, as we believe that the study of the unwavering resistance to expression in GroEL deficient *E. coli* exhibited by this chaperonin may require the implementation of methods beyond those used in the study of its

homologues.

CONCLUSION

Throughout the course of this study, we have observed an assortment of never before documented phenomena associated with ESKAPE pathogen GroEL. Though we have yet to conclusively verify the presence of conserved structural regions mutually targetable by small molecule inhibitors across *E. coli* and ESKAPE GroEL, our laboratory has obtained novel knowledge about the functional characteristics of the chaperonin in each of the former pathogenic organisms. It is our hope that through the continued investigation of ESKAPE pathogen GroEL within the *E. coli* model, we will conclusively identify structural and/or functional weaknesses shared among some of the most antibiotic-tolerant organisms on Earth, and ultimately develop successful pharmacological treatments for the infections which they invoke.

ACKNOWLEDGMENTS

I want to thank Dr. Eli Chapman, whose dedication to engaging undergraduate students in pragmatic, clinically relevant scientific investigations has facilitated my involvement in tactile microbiology, biochemistry, pharmacology, toxicology, and molecular and cellular biology. His adamancy for aiding others in understanding the natural world is remarkable, and I am truly proud and grateful to have been permitted to

play a part in experiments taking place within his laboratory.

I also thank Jared Sivinski for his unwavering patience throughout my learning of laboratory protocols and customs, his receptiveness to frequent questions, his thoroughly respective disposition towards myself and other individuals invested in scientific academia, and his incomparable willingness to teach others. In my eyes, Jared is the embodiment of an exceptional scientist, whose dedication to his craft has and continues to inspire me to pursue involvement in biological research. I am sincerely grateful for all of his guidance and mentorship, as well as aid in the composition of this Honors Thesis.

I would like to extend additional words of gratitude to; Andy Ambrose, Chris Zerio, Damian Mason, and Jason Machullis. Their willingness to answer my various inquiries regarding laboratory procedures has allowed me to thrive in the Chapman laboratory.

- Iliya Vitalievich Panfilenko

REFERENCES

1. Akers KS, Mende K, Cheatle KA et al. Biofilms and persistent wound infections in the United States military trauma patients: a case-control analysis. BMC Infect. Dis 2014;14(190):1-11.

2. Sirijan Santajit and Nitaya Indrawattana. Mechanisms of Antimicrobial Resistance in ESKAPE Pathogens. Biomed Res Int 2016; 2475067.

3. Singh S, Signh SK, Chowdhury I et al. Understanding the Mechanism of Bacterial Resistance to Antimicrobial Agents. Open Microbiol J. 2017;11:53-62.

4. Chapman E, Farr GW, Usaite R, et al. (2006). Global aggregation of newly translated proteins in an *Escherichia coli* strain deficient of the chaperonin GroEL. PNAS 103(43):15800-15805.

5. O. Keskin, I. Bahar, D. Flatow, D. G. Covell, and R. L. Jernigan. (2002) Molecular Mechanisms of Chaperonin GroEL-GroES Function. Biochemistry; 41:492-493.

6. Arthur L. Horwich, Wayne A. Fenton, Eli Chapman, George W. Farr. (2007) Two Families of Chaperonin: Physiology and Mechanism. Cell and Developmental Biology; 23:119.

7. Ranson NA, Farr GW, Roseman AM, Gowen B, Fenton WA, et al. 2001. ATP bound states of GroEL captured by cryo-electron microscopy. Cell 107:869–79

8. Xu Z, Horwich AL, Sigler PB. 1997. The crystal structure of the asymmetric GroEL-GroES-(ADP)7 chaperonin complex. Nature 388:741–50

9. Rye HS, Burston SG, Fenton WA, Beechem JM, Xu Z, et al. 1997. Distinct actions of cis and trans ATP within the double ring of the chaperonin GroEL. Nature 388:792–98

10. Horwich AL, Low KB, Fenton WA, Hirshfield IN, Furtak K (1993). Folding in vivo of bacterial cytoplasmic proteins: Role of GroEL. Cell 74:909–917

11. Chapman E, Farr GW, Fenton WA, Johnson SM, Horwich AL. (2008). Requirement for binding multiple ATPs to convert a GroEL ring to the folding-active state. PNAS 105(49):19205-19210

12. Santosh Kumar CM, Khare G, Srikanth CV, et al. (2009). Facilitated Oligomerization of mycobacterial GroEL: Evidence for phosphorylation-mediated oligomerization. J. Bacteriol. 191(21):6525-6538

13. Koike-Takeshita, A., Mitsuoka, K., & Taguchi, H. (2014). Asp-52 in Combination with Asp-398 Plays a Critical Role in ATP Hydrolysis of Chaperonin GroEL*. *The Journal of Biological Chemistry, 289*(43), 30005-30011.

14. Fukui N, Araki K, Hongo K, et al. (2016). Modulating the effects of the bacterial chaperonin GroEL fibrillogenic polypeptides through modification of domain hinge architecture. J. Biological Chemistry 291(48):25217-25226.

15. Motojima, F., Chaudhry, C., Fenton, W.A., Farr, G.W., & Horwich, A.L. (2004). Substrate polypeptide presents a load on the apical domains of the chaperonin GroEL. *Proceedings of the National Academy of Sciences of the United States of America, 101*(42), 15005-15012.

16. Ivic A, Olden D, Wallington EJ, Lund PA (1997). Deletion of *Escherichia coli groEL* is complemented by a *Rhizobium leguminosarum groEL* homologue at 37°C but not 42°C. Gene 194:1-8

17. Chen DM, Madan D, Weaver J, et al. (2013). Visualizing GroEL/ES in the act of encapsulating a folding protein. Cell 153(6):1354-1365.

18. Chen J, Smith DL. (2000). Unfolding and disassembly of the chaperonin GroEL occurs via tetradecameric intermediate with a folded equatorial domain. Biochemistry 39(15):4250-4258.

19. Horwich, A.L., Farr, G.W., & Fenton, W.A. (2006). GroEL−GroES-Mediated Protein Folding. *American Chemical Society, 2006*(106, 5), 1917-1930.

SUPPLEMENTARY FIGURES AND TABLES

Figure S4. *S. aureus* partial knock-in by lambda red recombination of *S. aureus* insertion cassette with MG1655 or MG*ΔgroESL*::EF *groESL* results in C terminal replacement. Clustal Omega protein sequence alignment of SA GroESL, FA GroESL, and partial SA knock-in to MG*ΔgroESL*::EF *groESL*. SA knock-in reversion to EF denoted at leading front of red-dashed box. Thirty-four base pair overlap between SA and EF *groESL* observed near reversion site

Bacterium	*Enterococcus faecium*	*Staphylococcus aureus*	*Klebsiella pneumoniae*	*Acinetobacter baumannii*	*Pseudomonas aeruginosa*	*Enterobacter cloacae*	*Escherichia coli*
Enterococcus faecium	-	69	58.6	57.9	59.2	58.1	58.4
Staphylococcus aureus	69	-	55.2	54.6	56.3	55.3	55
Klebsiella pneumoniae	58.6	55.2	-	73.7	77.2	98.4	95.8
Acinetobacter baumannii	57.9	54.6	73.7	-	76.4	72.3	73.1
Pseudomonas aeruginosa	59.2	56.3	77.2	76.4	-	76.4	76.7
Enterobacter cloacae	58.1	55.3	98.4	72.3	76.4	-	95.8
Escherichia coli	58.4	55	95.8	73.1	76.7	95.8	-

Table S2. MG1655 GroESL shares high amino acid identity with GroESL from the ESKAPE pathogens.

A

Bacterium	*Enterococcus faecium*	*Staphylococcus aureus*	*Klebsiella pneumoniae*	*Acinetobacter baumannii*	*Pseudomonas aeruginosa*	*Enterobacter cloacae*	*Escherichia coli*
Enterococcus faecium	-	83.5	75.5	76	76.1	75.5	75.2
Staphylococcus aureus	83.5	-	74.5	75.5	74.3	74.2	74
Klebsiella pneumoniae	75.5	74.5	-	85.6	87.4	99.5	98
Acinetobacter baumannii	76	75.5	85.6	-	88.1	85.6	85.4
Pseudomonas aeruginosa	76.1	74.3	87.4	88.1	-	87.3	87.3
Enterobacter cloacae	75.5	74.2	99.5	85.6	87.3	-	98
Escherichia coli	75.2	74	98	85.4	87.3	98	-

B

Bacterium	*Enterococcus faecium*	*Staphylococcus aureus*	*Klebsiella pneumoniae*	*Acinetobacter baumannii*	*Pseudomonas aeruginosa*	*Enterobacter cloacae*	*Escherichia coli*
Enterococcus faecium	-	75.3	62.9	66	70.1	62.9	62.9
Staphylococcus aureus	75.3	-	66	67	66	63.9	62.9
Klebsiella pneumoniae	62.9	66	-	77.6	76.3	100	97.9
Acinetobacter baumannii	66	67	77.6	-	86.7	77.6	78.6
Pseudomonas aeruginosa	70.1	66	76.3	86.7	-	77.3	78.4
Enterobacter cloacae	62.9	63.9	100	77.6	77.3	-	97.9
Escherichia coli	62.9	62.9	97.9	78.6	78.4	97.9	-

C

Bacterium	*Enterococcus faecium*	*Staphylococcus aureus*	*Klebsiella pneumoniae*	*Acinetobacter baumannii*	*Pseudomonas aeruginosa*	*Enterobacter cloacae*	*Escherichia coli*
Enterococcus faecium	-	84.9	77.7	77.8	77.1	77.7	77.4
Staphylococcus aureus	84.9	-	75.8	77	75.8	75.8	75.8
Klebsiella pneumoniae	77.7	75.8	-	87	89.4	99.5	98
Acinetobacter baumannii	77.8	77	87	-	88.3	87	86.7
Pseudomonas aeruginosa	77.1	75.8	89.4	88.3	-	89.1	88.9
Enterobacter cloacae	77.7	75.8	99.5	87	89.1	-	98
Escherichia coli	77.4	75.8	98	86.7	88.9	98	-

Table S3. GroESL protein identity (%) generated from EMBOSS Needle protein alignment of MG1655 GroESL and GroESL from the ESKAPE pathogens. Gram negative pathogens (*K. pneumoniae, A. baumannii, P. aeruginosa, E. cloacae*) share highest GroESL identity to *E. coli*. Likewise, gram positive pathogens (*E. faecium, S. aureus*) share higher identity with one another when compared to gram negative pathogens. Color gradient demonstrates highest identity highlighted in red, lowest identity in white.